Building Simulation 2009

*Eleventh International IBPSA Conference*
**Glasgow, Scotland**
**July 27-30, 2009**

# SELF-CALIBRATION AND OPTIMAL CONTROL OF A DOUBLE-SKIN SYSTEM

Seong-Hwan Yoon[1], Cheol-Soo Park[1], Godfried Augenbroe[2], and Deuk-Woo Kim[1]
[1]Dept. of Architectural Engineering, SungKyunKwan University, Suwon, South Korea
[2]Ph.D. program, College of Architecture, Georgia Institute of Technology
Atlanta, GA, U.S.A.
E-mail: cheolspark@skku.ac.kr

## ABSTRACT

To reduce the potential problems of window systems such as undesired heat gain (loss), glare, and thermal discomfort due to asymmetric radiation, double-skin systems have been introduced. The current problem with double skin systems is that their operation requires an adequate simulation model to realize optimal control of the system. The estimation of the parameters in the lumped model developed in a previous study (Park et al 2004a) was based on 'laborious' off-line calibration procedure. This effort has to be repeated for every different size, different type, or differently oriented façade system. Different façade components are characterized by different thermal and optical properties of glazing and louvers, system configurations [height, width, depth], other simulation variables, etc. For each type the parameter set in the lumped model has to be established through a calibration procedure. In view of micro climate variations even same type systems within one façade but on different heights may have to be calibrated separately. In order to avoid the laborious off-line calibration of every single façade component, an online self-calibrating procedure is developed in this paper. The true advantage of the technique is that every component can be pre-wired and ready to be hooked to the calibration set-up when it is brought to the site. The paper will explain the simulation model, selection of calibration parameters, and the process of on-line self-calibration, model validation and application of optimal control. It is shown that the on-line self-calibrating simulation model far outperforms the off-line calibrated model. Consequently, the plug and play self-calibration technique will render the current *in-situ* 'laborious' off-line calibration process obsolete.

## INTRODUCTION

Concerns about the earth's environment such as the depletion of fossil fuels, global warming, and greenhouse gas have stimulated the effort of reducing building energy use. As a part of these efforts to save energy, there have been many studies on optimal HVAC system control and Building Energy Management System (BEMS) control (Wang et al., 2000; Chow et al., 2001; Nassif et al., 2005; Wen et al, 2007). Even though these efforts help to minimize building energy use, they cannot lessen the excessive heat gain (loss) through the building envelope. Therefore, in order to reduce the total energy use, there should be a way to reduce heating/cooling load from the building envelope. In particular, transparent envelopes that should be carefully designed due to high U-values. A double-skin system can be a solution to the aforementioned issues and has already been applied to many buildings.

The current problem of a double-skin system is that the applied control is not model-based dynamic control but a straightforward rule-based control (CIBSE 1996). The model-based dynamic control provides more accurate and better control since it is based on the predicted response of the system. In order to achieve the dynamic control, a simple model but accurate enough is required.

Hence, the objectives of the paper are (1) to develop a self-calibrating simulation model required for optimal control, and (2) using the model, to achieve the real-time optimal control of a double-skin system. To accomplish the aforementioned objectives, it is necessary to have: (1) an underlying mathematical model to describe the complicated physical phenomena, (2) an estimation of the unknown parameters introduced during the modeling process and model simplification, (3) development of a cost function for optimal control, and (4) solving for optimal control variables.

Predictions of the system's dynamic response are influenced by the following: (1) assumptions introduced during the modeling process, (2) unmodeled physical phenomena (e.g., heat transfer and airflow distribution in a corner of a system, infiltration through the ventilation dampers, etc.), and (3) parameters that are not observable or impossible to solve analytically. Park et al. (2004a) introduced an off-line parameter estimation technique to calibrate the simulation model numerically and solve the aforementioned problems. The 'calibrated model with off-line parameter estimation' is much more accurate than the 'uncalibrated model', but off-line calibration has the following problems:

- Laborious experiments, tedious parameter estimation, and model validation process: depending on the airflow regime of the double-skin system, weather condition

(outdoor temperature, wind direction, and speed), and indoor condition, the three processes should be executed (modeling, parameter estimation, and validation).

- Changes in the system configuration: the simulation model requires recalibration if the system configuration (depth and height of the cavity, type and thickness of glazing, reflectance and absorptance of louver slat, etc.) changes (Yoon et al., 2007). In other words, the process of remodeling, calibration, and validation is required to design and apply for a new system configuration.
- Changes in physical properties over time: For example, in mobile robotics, wear and tear can change the diameter of wheels and loosen belts. The following physical properties of the system can change such as transmittance and reflectance of glazing, reflectance of louver surface due to accumulated dirt, and so on. To reflect such changes, regular model calibration and validation are required, which is not easy with off-line calibration.

Therefore, the paper introduces a self-calibration technique for the simulation model. The self-calibrating model developed in this study constantly updates the model based on information (input variables, state variables) from sensors. The paper compares the self-calibrating model with the off-line model reported in (Park et al 2004a). Furthermore, the result of real-time optimal control simulation using the self-calibrating model is also addressed in the paper.

## EXPERIMENTAL SET-UP

An experimental test facility was constructed as shown in Figure 1. The test facility is true south facing, and consists of a single pane exterior glazing (6mm low-e), a double pane interior glazing (6 mm clear [outer glazing] + 12 mm air space + 6mm low-e [inner glazing]), an automatic rotating louver (5 cm wide, black PVC, centered in the cavity), and electrically controlled ventilation inlet/outlet dampers (0.25 m high, 2 m wide) at the top and bottom of each glazing layer (Figure 2). The test unit is constructed that multiple configurations of the system can be tested, e.g., inside window (low-e vs. clear), cavity depth (250 mm vs. 400 mm) and louver color (black, white, and ivory).

(a) exterior (b) interior

*Figure 1. The test unit (installed in Sungkyunkwan University campus, Korea)*

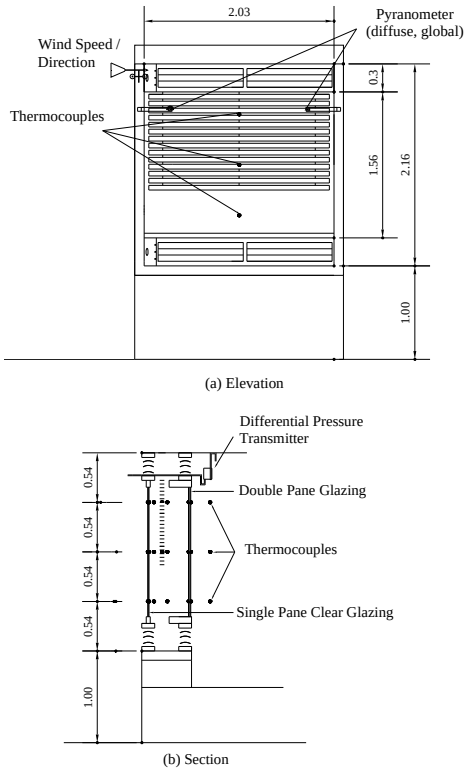


*Figure 2. Elevation and section of the experiment unit showing the location of sensors*

Sensors and measuring instruments (Figure 2) include: an HOBO weather station (H21-001) and Omega T-type thermocouples to record solar radiation, wind velocity, and temperatures at various locations. The cavity air velocity is measured with a TESTO hot sphere anemometer (T-06995100) located at a point about 100 cm above the bottom.

## MATHEMATICAL MODEL

In order to develop the mathematical model of a double-skin system, the governing heat and mass transfer phenomena are studied: (1) direct, diffuse, and reflected solar radiation, (2) long wave radiation between surfaces, (3) convective heat transfer along exterior glazing, interior glazing, and louver slats, and (4) air movement through inlet/outlet dampers and the cavity.

The system involves transient heat transfer and turbulent air flows in irregular 3D geometry with

boundary conditions constituted by outside temperature and solar radiation, etc. In addition, while actually simulating the dynamics of the system, adequate optimal control actions must be determined in real-time, effects of which are dynamically coupled with the dynamics of the system of a highly nonlinear nature. Thus, in order to describe the dynamics of the system solvable with reasonable efforts, the lumped physical model had to be developed as follows: By assuming the heat transfer in the lateral direction to be negligible, the thermal behavior of the system can be reduced to a 2D model (Figure 3). Next, we lump the exterior glazing temperature, the interior glazing temperature, the louver temperature, and the cavity air temperature in the vertical direction. Although this cannot render the explicit vertical temperature gradients, this lumping is assumed to have little effect in representing the overall thermal characteristics of the system and on determining optimal control actions. This has, of course, to be substantiated by experiments and will be described later in the paper. Since the details of the lumped model are provided in Park et al. (2004a), the paper addresses it briefly as follows.

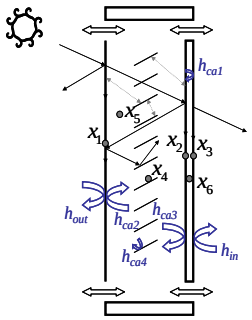


*Figure 3. Simplified system in 2D (•: state variables, $x_1$=exterior glazing temperature, $x_2$=outer glazing temperature of the interior double-pane, $x_3$= inner glazing temperature of the interior double-pane, $x_4$=louver slat temperature, $x_5$=air temperature in the larger cavity, and $x_6$=cavity air temperature in the interior double-pane)*

The simulation model consists of a thermal model (states variables, Figure 3) and a cavity airflow model. In the thermal model, we used the fictitious cavity suggested by Rheault et al. (1989) to formulate the long wave and short wave radiation between surfaces.

In the modeling of the convective heat transfer, the six convective heat transfer coefficients ($h_{out}$, $h_{ca,1}$, $h_{ca,2}$, $h_{ca,3}$, $h_{ca,4}$, $h_{in}$) as shown in Figure 3 should be estimated because the literature values of those coefficients (ASHRAE, 2005; Clarke, 2001; Incropera et al., 2003; ISO, 199; McAdams, 1954) are empirically driven for general cases and thus, can significantly vary according to the wind direction and speed, airflow regime in the cavity, surface roughness, system configuration and location, surroundings, micro-climate, etc.

The remainder of this section will concentrate on the modeling of air movement through the inlet/outlet dampers. Firstly, ten possible airflow regimes have been selected (Figure 4). In Mode #1-2 the interior upper and lower dampers are open (inside circulation) and Mode #3-4 are reversed (outside circulation). For Mode #1-2, air circulation between the room and the cavity is driven by thermal buoyancy while in Mode #3-4, air circulation is driven by thermal buoyancy and wind pressure. Mode #5-8 allow a diagonal airflow either from inside to outside or vice versa. Mode #9 and #10, respectively, represent the cases where the four dampers are open/closed. The mathematical equations to express the airflow are provided in detail by Park et al. (2004a).

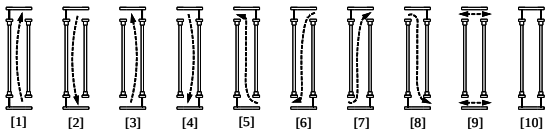


*Figure 4. Ten airflow regimes (louver slats not drawn for clarity)*

Based on what has been provided above, the mathematical model is expressed with a continuous state-space equation as shown in Equation (1).

$$\dot{x} = A(u,t)x + b(u,t) \tag{1}$$

It should be noted that the room or the building model is not part of the self-calibrating model, which means that the double-skin facade system is treated as a 'local' system and hence, based purely on local state information. The benefit of isolating the self-calibrating model is that the resulting double skin component with its embedded optimal control can become a part of any building model. If the double-skin system needs to be incorporated into a room or a building model, a set of differential equations for other states such as door, ceiling, and walls can be added to Equation (1) for a simultaneous solution.

Note that the dependency of $A$ on $u$ results in a system that is nonlinear in $u$. This is prohibitive to a numerical state space solution. By converting the continuous (in time) state space (1) to a discrete (in time) state space, Equation (2), this nonlinearity disappears because $u_k$ = constant for $t_k \le t \le t_{k+1}$.

$$x((k+1)T) = G(T)x(kT) + H(T) \tag{2}$$

where $G(T) = e^{AT}$ , $H(T) = A^{-1}(e^{AT} - I)b$ and $T$ is the sampling time.

## SELF-CALIBRATION

Modeling is the process of mathematically describing the physical behavior of the system (usually in the form of a set of differential equations). The model carries a set of unknown parameters that need to be determined such that the lumped model describes the real behavior as closely as possible. As discussed in (Park et al. 2004a), the most noticeable unknown

parameters in the lumped model include the convective heat transfer coefficients (Figure 3), the form loss factor (*f*) for Modes #1-#2 (Figure 4), the flow coefficient (*c*) and exponent (*n*) for Modes #5-#8. These parameters cannot be measured directly and are impossible to analytically derive. For these reasons, a self-calibration technique is introduced. The self-calibration technique, one of the parameter estimation techniques, is the on-line real-time process of calculating unknown parameters for a system which minimize the deviation between model output and measurement output. This can be formulated into minimizing an objective function S over the measurement period as follows:

$$\min S = \sum_{k=1}^{z} \lambda^{z-k} [Y_k - \psi_k(\xi_i)]^T [Y_k - \psi_k(\xi_i)] \qquad (3)$$
$$s.t.: lb \le \xi \le ub$$

Where $\lambda$ is a time-varying weighting vector designed to give higher weight to later data values than earlier values. Thus, the later data has more of an impact on the parameter estimation.

The real time calibration provides the reliability of the simulation model and accurate prediction of the system's response. The unknown parameters are estimated as shown in Figure 5.

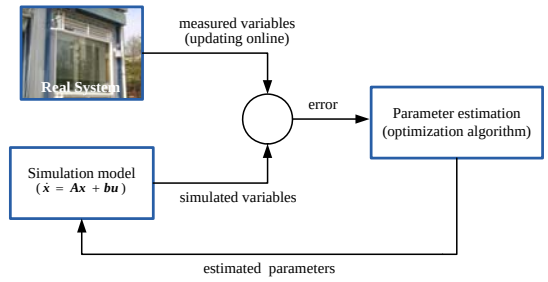


*Figure 5. Architecture of the Self-calibrating model*

The double-skin model expressed in Equation (1) is constructed by coupling the thermal model and airflow model, using the ping-pong method where the thermal and airflow models are run in sequence (Hensen, 1999) (Figure 6).

## OPTIMAL CONTROL

The performance of a double-skin system can be categorized into the following elements: energy use, visual comfort, thermal comfort, and ventilation performance. In this paper, we deal with an energy element, and the cost function *J* is formulated as follows:

$$J_{heat} = -\int_{t_1}^{t_2} (Q_{cv,rd} + Q_{sol,trans} + Q_{air} + Q_{DA}) dt \qquad (4)$$

$$J_{cool} = \int_{t_1}^{t_2} (Q_{cv,rd} + Q_{sol,trans} + Q_{air} - Q_{DA}) dt \qquad (5)$$

The optimal control attempts to find the control variables which minimize the cost function (*J*) over a certain period of time as shown in Equation (6); 15 minutes was used as a time horizon in this study.

$$\begin{aligned} &\min J(\phi, AFR, OR) \\ &s.t. -90^\circ \le \phi \le 90^\circ \\ &AFR = 1,2,3,4,5,6,7,8,9,10 \\ &0 \le OR \le 100\,(\%) \end{aligned} \qquad (6)$$

Due to the nonlinearity of the system dynamics and additional constraints on the control variables shown in Equation (6), it is difficult to find the optimal solution. Additionally, the optimization problem consisting of continuous control variables ($\phi$, *OR*) and discrete control variables (*AFR*, Figure 4) leads to a combinatorial problem, which is unrealistic to solve (Winston, 1994). Thus, the discrete airflow regime (*AFR*) is translated as a continuous variable (*AFR**) (Park et al., 2004b).

Then, to perform the on-line optimal control, the VI 'Constrained Nonlinear Optimization', one of the LabVIEW optimization routines and NI Data Acquisition Hardware are coupled. The VI 'Constrained Nonlinear Optimization' solves a general nonlinear optimization problem with nonlinear equality and inequality constraint using a sequential quadratic programming method.

## RESULTS

### Self-calibration

The airflow model experiment was done on December 8th-11th, 2008 with a measurement sampling interval of 1 minute (datapoints: 4,619). During the experiment, the louver angles and the airflow regimes were randomly changed, as shown in Figure 7(a). Figure 7(b) shows the cavity air velocity calculated from the self-calibrating model, off-line calibration model, with the measured one. As shown in Figure 7(b), the self-calibrating model proved surprisingly accurate.

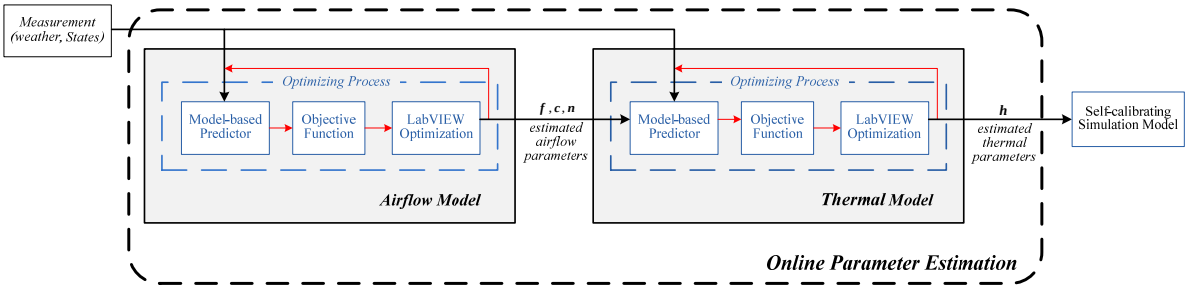


*Figure 6.The self-calibrating process*

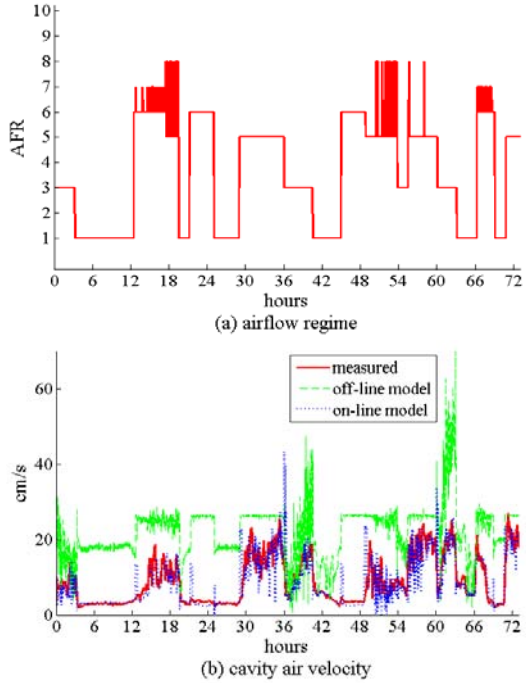


*Figure 7. Comparison of cavity air velocity*

Table 1 shows the average difference in the cavity air velocity between the measured data and the off-line calibration model and between the measured data and the self-calibrating model at each airflow mode (Figure 4). It is shown that a self-calibrating model is far accurate due to the following: (1) state variables ($x_1$-$x_6$, Figure 3) are updated in real-time that are used for the prediction of air velocity, and (2) the model recalibration updates the unknown parameters continuously.

*Table 1*

*Average of difference in the cavity air velocity*

| AIR FLOW REGIME | DIFFERENCE BETWEEN MEASURED AND OFF-LINE CALIBRATION MODEL | DIFFERENCE BETWEEN MEASURED AND SELF-CALIBRATING MODEL | AVERAGE OF MEASERED CAVITY VELOCITIY |
|---|---|---|---|
| [1] | 12.71cm/s | 0.50 cm/s | 2.76 cm/s |
| [3] | 11.56 cm/s | 2.76 cm/s | 10.16 cm/s |
| [5] | 11.41 cm/s | 3.24 cm/s | 14.10 cm/s |
| [6] | 19.21 cm/s | 2.01 cm/s | 5.72 cm/s |

The thermal model experiment (thermal model) was conducted on the 5th-8th (closed cavity) and 8th-11th (open cavity) of December 2008 with a measurement sampling interval of 1 minute during which 4,394 (about 3.0 days or 73.2 h) and 4,619 data points (about 3.2 days or 76.9 h) were obtained, respectively. Due to limited space, only weather and the simulation results of the closed cavity are shown in Figures 8-9, but the results of the open cavity are similar. It should be noted that the state variable $x_6$, corresponding to the small cavity in the interior double-pane, was not measured.

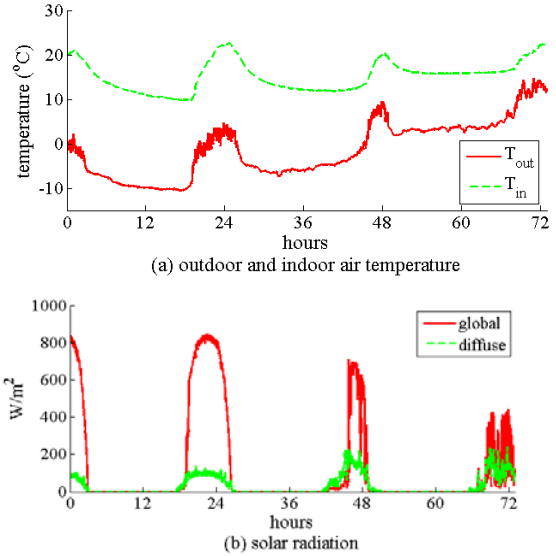


*Figure 8. Weather during the experiment of the closed cavity (12/05/2008-12/08/2008)*

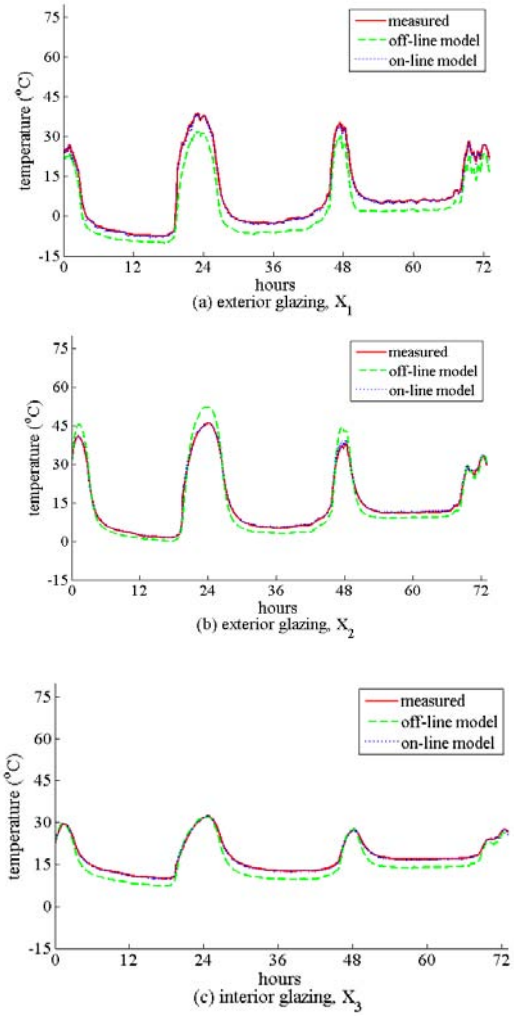

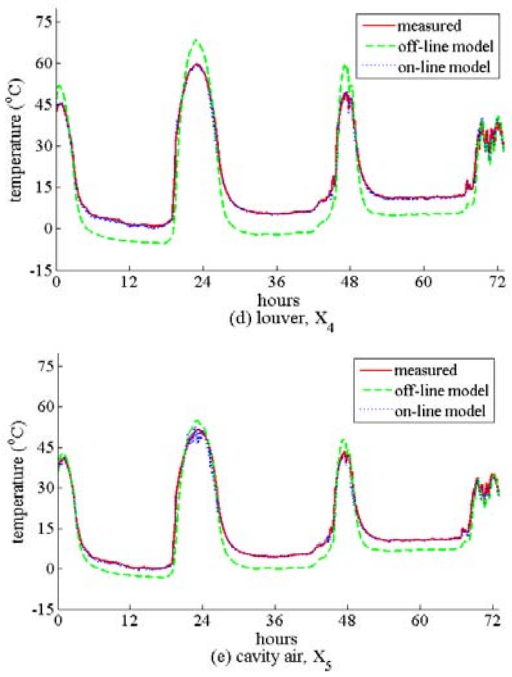


*Figure 9. Simulation results of state variables*

As shown in Figure 9, prediction by the real-time self-calibrating model nearly overlaps the measured data and can predict the system response accurately compared to the results of the off-line calibration model. Table 2 shows the average of differences between predictions of the simulation models (both off-line and on-line) and measured data, in closed and open cavity conditions.

*Table 2*

*Average of difference in state variables*

| STATE VARIABES | AVERAGE OF DIFFERENCE BETWEEN MEASURED AND OFF-LINE | AVERAGE OF DIFFERENCE BETWEEN MEASURED AND SELF-CALIBRATING | AVERAGE OF MEASURED STATE VARIABLES |
|---|---|---|---|
| $x_1$ | 4.75°C | 0.56°C | 7.52°C |
| $x_2$ | 1.03°C | 0.39°C | 14.89°C |
| $x_3$ | 2.34°C | 0.25°C | 17.70°C |
| $x_4$ | 4.92°C | 0.51°C | 17.03°C |
| $x_5$ | 3.24°C | 0.64°C | 15.00°C |
| *average* | 3.26°C | 0.47°C | 14.43°C |

**Real-time optimal control**

Real-time optimal control simulation runs were conducted during separate winter days, totally for 50 hours or 4 days (12/30/2008, 01/05/2009 – 01/07/2009) as shown in Table 3. During holidays and nighttimes, the optimal control experiments were not conducted. A sampling time of 1 minute was used and the number of recorded data points was 3,060. Figure 10 shows the state variables, outdoor temperature and solar radiation during the experiment.

*Table 3*

*Five separate optimal control simulation runs*

| | START | END | NUMBER OF DATA POINTS |
|---|---|---|---|
| 1st | Dec. 29 11:51 A.M. | Dec.30 7:05 P.M. | 300 (6.1h) |
| 2nd | Dec.30 7:05 P.M. | Dec.30 7:05 P.M. | 200 (3.3h) |
| 3rd | Dec.30 7:05 P.M. | Dec.30 7:05 P.M. | 400 (6.6h) |
| 4th | Dec.30 7:05 P.M. | Dec.30 7:05 P.M. | 753 (12.5h) |

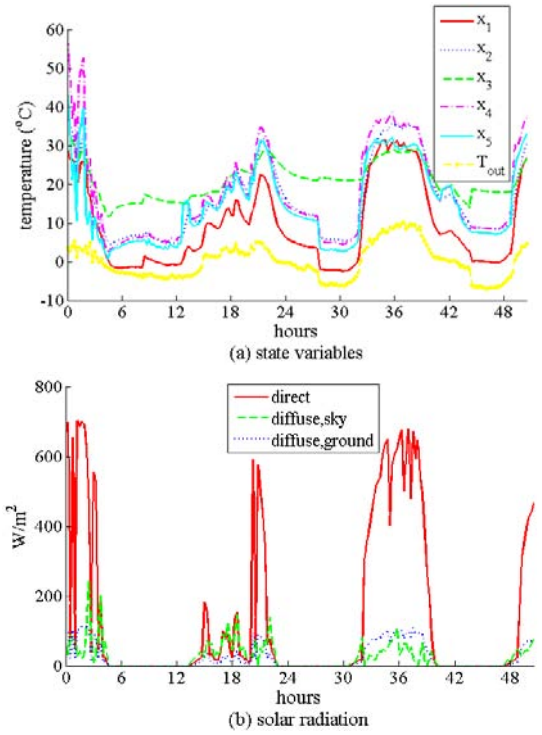


*Figure 10. Measured state variables and weather conditions*

Figure 11 shows the optimal control variables. Figure 11(a) includes the optimal control louver angle ($\phi$), the actual driving louver angle ($\phi$ *), and solar altitude (sol.alt). In order to solve Equation (6), the louver slat angle is considered as a continuous control variable, but the actual louver slat installed in the experimental unit (Figure 1) cannot be controlled continuously. The possible minimum operation interval of the louver slat angle by an installed motor is 18˚. Therefore, in this study, the continuous louver slat angle was rounded to a nearest multiple of 18˚.

Figure 11(b) and (c) shows the optimal airflow regime (*AFR*) and optimal opening ratio of the ventilation damper (*OR*), respectively.

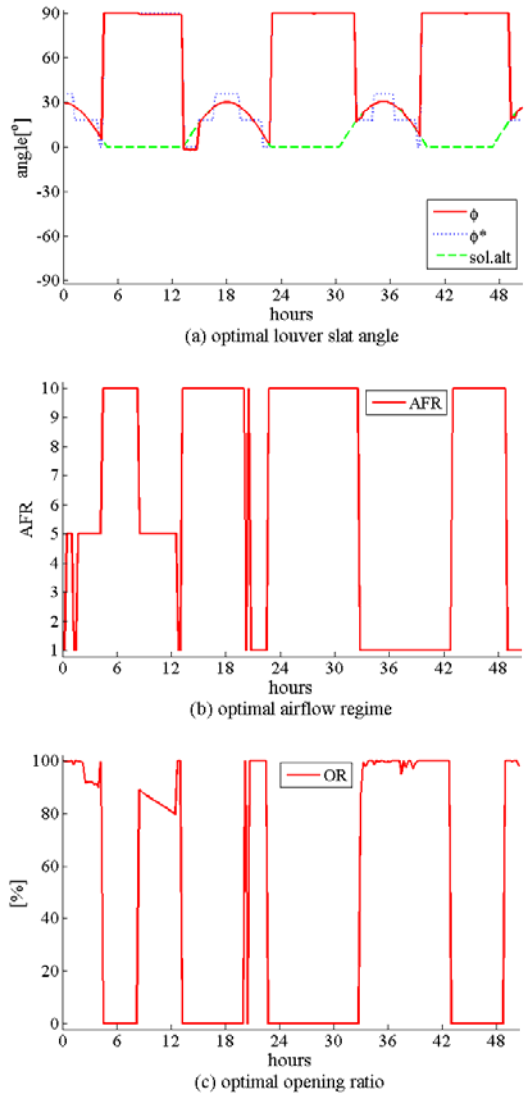


*Figure 11. Results of real-time optimal control simulation: heating mode (winter day)*

Figure 11(a) shows that the optimal louver slat angle keep track of the solar altitude so that it can absorb direct solar radiation during daytime. At nighttime, the louver slat angle stays at 90˚ such that it can reduce heat loss by long wave radiation between the interior glazing and the colder exterior glazing.

In addition, the optimal louver slat angle was maintained at a vertical position (90˚) after sunrise (hours between 30 and 32, between 47 and 49 in Figure 11(a)) by influence of a high-rise apartment located east of the experiment unit. However, on the second day of the experiment (hours between 10 and 27 hours), the optimal louver slat angle was calculated between -1.6˚ to -2˚ after sunrise (hours between 13 and 15). It is assumed that absorbing the solar radiation is better for saving energy than reducing the the heat loss through long wave radiation by maintaining a louver slat angle of 90˚.

As shown in Figure 11(b), the optimal airflow regime during daytime is inside circulation (Mode 1, Figure 4) with a clear sky and closed cavity (Mode 10, Figure 4) or diagonal airflow (Mode 5, Figure 4) with an overcast sky. It can be inferred that it reduces heating energy use using the hot cavity air under a clear sky and reduces transmission heat loss using exhaust air to heat the cavity under an overcast sky. As supply of outdoor air as well as exhaust of contaminated indoor air are required, exhausting the indoor air through the cavity can reduce both return air fan power and heat loss through building envelope.

The optimal airflow regime at night (when solar altitude is 0˚ in Figure 11(a)) is similar to that of daytime under an overcast sky. In the second day simulation (hours between 10 and 27 hours), the operation of optimal airflow regime is clearly shown (Figure 11(b)). The sky condition changed from an overcast to a clear sky (around hour 20). At that time, the optimal airflow regime also changed from the closed cavity (Mode 10, Figure 4) to inside circulation (Mode 1, Figure 4) so as to use the hot cavity air.

The ventilation dampers are almost fully open except when the airflow regime is closed to utilize the hot cavity air.

## CONCLUSION

In the paper, a real-time self-calibrating model procedure has been developed and its role in the optimal control of a double skin system has been demonstrated. The lumped model that simplifies the 3D physical phenomena was introduced. It contains a set of unknown parameters that can be calibrated real time, by minimizing the difference between measured and simulated values. Over time a recalibration can be done repeatedly, in the same manner. In this study, the on-line self-calibrating model proved more accurate in the prediction of system's response than the off-line calibration model. In particular, the prediction of the self-calibrating model is surprisingly accurate. In addition, the real-time optimal control based on the self-calibrating model determines the optimal control actions effectively. Based on these findings, the use of pre-wired, plug and play façade components is a feasible option for the large scale application of optimally controlled double skin façade systems.

Based on the results of this study, the following studies are on-going: (1) Performance assessment of thermal comfort, visual comfort, and ventilation, (2) Integration of the double-skin system with a buildings' HVAC system, (3) Ubiquitous web-enabled optimal control of plug and play components of a double skin system.

## REFERENCES

Aström, K.J and Wittenmark, B. 1995. Adaptive Control, Addison-Wesley Publishing Conpant, Inc.

Chow, T.T., Lin, Z. and Song, C.L. 2001. Applying neural Network and Genetic Algorithm in Chiller System Optimization, Proceedings of the 7th IBPSA Conference (International Building Performance Simulation Association), August 13-15, Rio de Janeiro, Brazil, pp.1051-1065

CIBSE 1996. City Slicker, CIBSE Journal, vol.18, no.9, pp.20-24

Clarke, J.A. 2001. Energy Simulation in Building Design, Butterworth-Heinemann, 2nd Ed.

Donald, E.K. 2004. Optimal Control Theory, Dover Publications, Inc.

Hensen, J. 1999. A Comparison of Coupled and Decoupled Solution for Temperature and Air flow in a Building, ASHRAE Transactions, vol.105, pp.962-969

Incropera, F.P. and DeWitt D.P. 2003. Fundamentals of Heat and Mass Transfer, John Wiley&Sons, 5th Ed.

ISO 1999. Thermal Performance of Windows, Doors and Shading Devices – Detailed Calculation, ISO TC 163

Lewis, F.L. and Syrmos, V.L. 1995. Optimal Control, John-Wiley&Sons, Inc. 2nd Ed.

McAdams, W.H. 1954. Heat Transmission, New York: McGraw-Hill

Nassif, N., Kajl, S. and Sabourin, R. 2005. Simplified Model-based Optimal Control of VAV Air-conditioning System, Proceedings of the 9th IBPSA Conference (International Building Performance Simulation Association), August 15-18, Rio Montreal, Canada, pp.823-830

Oesterle, E., Lieb, R,D. and Lutz, M. 2001. Double-Skin Facades, Prestel

Park, C.S. and Augenbroe, G., Messadi, T., Thitisawat, M. and Sadegh, N. 2004a. Calibration of a lumped simulation model for double-skin facade systems, Energy and Buildings, vol36, pp.1117-1130

Park, C.S. and Augenbroe, G., Sadegh, N., Thitisawat, Mate. And Messadi, T. 2004b, Real-time optimization of a double-skin facade based on lumped modeling and occupant preference, Building and Environment, vol.39, pp.939-948

Rheault, S. and Bilgen, E. 1989. Heat Transfer Analysis in an Automated Venetian Blind Window System, Journal of Solar Energy Engineering, vol.111, no.1, pp.89-95

Saelens, D. 2002. Energy performance assessment of single story multiple-skin facades, Ph.D. Dissertation, Katholieke Universiteit Leuven

Sealens, D., Roels, S. and Hens, H. 2008. Strategies to improve the energy performance of multiple-skin facades, Building and Environment, vol.43, no.4, pp.638-650

Wang, S.W. and Jin, X.Q. 2000. Model-based optimal control of VAV air-conditioning system using genetic algorithm, Building and Environment, vol.35, pp.471-487

Wen, J. and Smith, T.F. 2007. Development and validation of online models with parameter estimation for a building zone with VAV system, Energy and Building, vol.39, pp.13-22

Wigginton, M. and Harris, J. 2002. Intelligent Skins, Elsevier

Winston, W.L. 1994. Ooerations research, Duxbury Press.

Yoon, S.H. and Park, C.S. 2007. State-space Approach for Lumped Modeling of Double-skin System, Proceedings of the Sustainable Building Conference 2007 Hong Kong (SB07 HK), December 3-5, Hong Kong, China

## NOMENCLATURE

| | |
|---|---|
| $x$ | state vector |
| $A$ | state matrix |
| $b$ | load vector |
| $u$ | control or input variables |
| $t$ | time |
| $Y_k$ | observation vector at time $k$ |
| $\psi_k$ | predicted vector of observations |
| $z$ | number of observation |
| $\xi$ | vector of unknown parameters |
| $lb$ | vectors of lower bounds of the parameters |
| $ub$ | vectors of upper bounds of the parameters |
| $J_{heat}$ | cost function in heating mode |
| $J_{cool}$ | cost function in cooling mode |
| $Q_{cv,rd}$ | heat gain in the room space by convection and radiation on the interior glazing |
| $Q_{sol,trans}$ | sum of transmitted direct and diffuse solar radiation |
| $Q_{air}$ | heat gain the room space by beneficial airflow regime from the cavity to the room space or outside |
| $Q_{DA}$ | energy savings by daylighting autonomy |
| $\phi$ | louver slat angle (0˚: horizontal, (0˚~90˚: towards the sky, -80˚~0˚: towards the ground) |
| $AFR$ | AirFlow Regime (Figure 4) |
| $OR$ | opening ratio of ventilation damper |